arXiv:astro-ph/0509423v2 19 Sep 2005

Evolution of Galaxies and the Tully–Fisher Relation

E. P. Kurbatov,[1, *] A. V. Tutukov,[1, †] and B. M. Shustov[1, ‡]

[1]*Institute of Astronomy, Moscow, Russia*

We study the evolution of the [O/Fe]–[Fe/H] relation and the dependence of the iron abundance on distance from the galactic plane z in a one-zone model for a disk galaxy, starting from the beginning of star formation [1]. We obtain good agreement with the observational data, including, for the first time, agreement for the [Fe/H]–z relation out to heights of 16 kpc. We also study the influence of the presence of dark matter in the galaxies on the star-formation rate. Comparison of the observed luminosity of the Galaxy with the model prediction places constraints on the fractional mass of dark matter, which cannot be much larger than the fractional mass of visible matter, at least within the assumed radius of the Galaxy, ~ 20 kpc. We studied the evolution of disk galaxies with various masses, which should obey the Tully–Fisher relation, $M \propto R^2$. The Tully–Fisher relation can be explained as a combination of a selection effect related to the observed surface brightnesses of galaxies with large radii and the conditions for the formation for elliptical galaxies.

I. INTRODUCTION

Many thousands of theoretical papers have been written on the evolution of galaxies, often applying sophisticated mathematical methods: N-body models, multidimensional gas-dynamical models, statistical methods etc. However, a number of very important results can be obtained using methods that are relatively simple and are not computationally demanding. In [1, 2, 3, 4, 5], we suggested and implemented an approach that is both simple mathematically and reasonably self-consistent in the treatment of all complex physical processes determining the evolution of a galaxy.

In mathematical terms, this evolution reduces to the solution of two equations. One defines the star-formation rate (SFR) assuming the complete ionization of the gas component of the galaxy, which is taken to be homogeneously distributed over the galactic disk. The other equation describes variations of the thickness of the galactic disk based on the condition of virial equilibrium, the input of mechanical energy into the gas component by supernovae, and the dissipation of energy due to collisions of gas clouds. Numerical modeling must also take into account the evolution of the galactic stellar component: the return of matter to the interstellar medium by old stars after the formation of the endproducts of their evolution — black holes, neutron stars, and degenerate dwarfs — and the exchange of matter between the galaxy and intergalactic medium.

Despite the simplicity of this approach, it led to a fairly complete picture of the evolution of disk galaxies — in particular, the Milky Way — that was consistent with observations. This made it possible for the first time to distinguish the role of the loss of heavy elements from the Galaxy during the formation of the radial chemical-composition gradient, and to derive self-consistent distributions of metals in the z direction over a scale of ~ 2 kpc. This provided an explanation for the origin of enhanced metallicities (by a factor of a few over the solar value) of galaxies harboring quasars in their nuclei, via the enhanced density and higher minimum mass of the stars in these regions [5].

---

[*] Electronic address: kurbatov@inasan.ru

[†] Electronic address: atutukov@inasan.ru

[‡] Electronic address: bshustov@inasan.ru

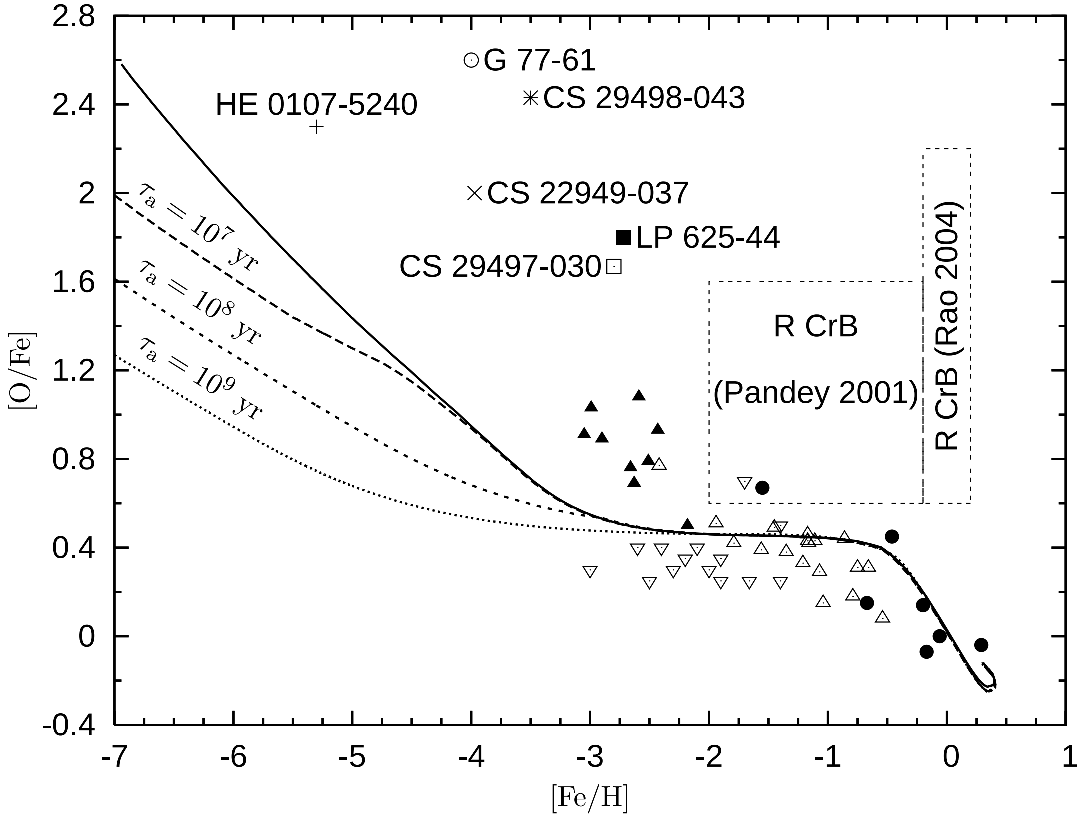

FIG. 1: [O/Fe]–[Fe/H] dependence for models with various initial accretion times τ_a. The solid curve shows the standard model ($\tau_a = 0$). The filled circles show data on subgiants [6], open triangles data on subgiants and main-sequence stars [7], filled triangles data on subdwarfs [8], inverted open triangles data on halo giants [9], and rectangles the positions of R CrB stars [10, 11]. The remaining objects are HE 0107-5240 [12], CS 22949-037 [13], CS 29498-043 [14], CS 29497-030 [14], LP 625-44 [14], and G 77-61 [15].

The present paper continues our study of the evolution of disk galaxies using the model developed by us earlier. This model enabled us to trace the chemical evolution of galaxies starting from their formation. However, the absence of data on very old, low-metallicity stars prevented comparison of the model results with observational data for the initial stages of the evolution of the Galaxy. New data for stars with extremely low metallicities has recently become available, making it possible to trace the early stages of the enrichment of the Galaxy in heavy elements. Section 2 discusses the evolution of abundances implied by our theoretical modeling. Section 3 discusses modern data on the distribution of metals in the direction of the Galactic rotational axis on scales of 16 kpc. In our previous studies, we used only fairly old data on stars that are located not further than 3 kpc from the disk — again hindering application of the model to the earliest stages of Galactic evolution. Another important circumstance influencing the evolution of the Galaxy is the presence of dark matter in the Galaxy. The nature and properties of dark matter are far from fully understood (see, e.g., the review [16]), but the necessity of taking this factor into account is beyond doubt. Section 4 presents an estimate of the fractional mass of dark matter obtained in our model.

The good agreement of the model results with the observations encourages us to use the model to interpret various statistical relations (mass–metallicity, mass–luminosity, etc.). In recent years, possibilities for applying the Tully–Fisher relation [17], which was discovered in 1977 by the two named authors, in various studies of galaxies have been widely discussed. This law relates the luminosity and rotational velocity of a disk galaxy. There are various ideas about the origin of the Tully–Fisher relation. In Section 5, we suggest an explanation that seems to us quite natural, based on an analysis of galactic evolution using our model. Finally, Section 6 presents a summary of our results.

We made some modifications to the set of standard parameters for the Galaxy for the computations; these are described in the corresponding Sections.

II. EVOLUTION OF THE OXYGEN AND IRON ABUNDANCES

Analyses of the oxygen and iron abundances are the classical methods for testing our understanding of the evolution of stars and galaxies. These elements were adopted as tools for directly analyzing the abundances of the products of type I supernovae (SN Ia, which produce mainly iron) and type II supernovae (SN II or SN Ib,c, which produce mainly oxygen). The time between the formation of a massive star and its explosion as a SN II or SN Ib,c does not exceed $\sim 10^7$ yr. According to one possible scenario, SN Ia result from the mergers of degenerate dwarfs [18]. The lifetimes of SN Ia precursors cover a wide range, from 10^7 to 10^{10} yr, with the most probable values being from 2×10^8 yr to 2×10^9 yr [19]. The possibility that SN Ia make a significant contribution to the production of iron in the Galaxy at ages lower than $\sim 10^9$ yr is supported by the discovery of an [O/Fe] ratio equal to the solar value in a distant quasar [20] with $z = 6.4$ (age $\sim 7 \times 10^8$ yr). We have used here a standard model for the evolution of the Galaxy: the closed model with outer radius $R = 20$ kpc and mass $M = 2 \times 10^{11} M_\odot$ described in [1]. The only difference is in the lifetime of SN Ia precursors (which was assumed to be 10^9 yr, close to the median value in the scenario for the evolution of close binaries [19]). In previous computations of the standard model [1], this time was taken to be 3×10^8 yr. Test runs have shown that this change does not result in any fundamental changes in the results of the computations; therefore, we shall adopt this modified model as our standard.

We considered the evolution of the [O/Fe]–[Fe/H] relation in a number of previous studies [1, 4, 5], using stars in the solar neighborhood with relative iron abundances $[\mathrm{Fe/H}] > -3$. The metallicity range considered here is wider, extending to $[\mathrm{Fe/H}] = -7$. The main results are presented in Fig. 1. When $[\mathrm{Fe/H}] < -1$, the abundances of oxygen and iron are determined primarily by SN II explosions, leading to an overabundance of oxygen by a factor of two to four. At an age of $\sim 5 \times 10^8$ yr, SN Ia begin to explode, producing primarily iron [21] (in the closed model, this age corresponds to $[\mathrm{Fe/H}] \approx -0.5$). The ratio [O/Fe] begins to decline with time (along with the increase of [Fe/H]), and approaches the solar value at an age of several Gyr. The model provides an acceptable distribution for most stars with $[\mathrm{Fe/H}] > -3$.

Among stars with the solar abundance of heavy elements, it has long been known that R CrB stars have abnormally high abundances of oxygen and carbon. The positions of R CrB stars with solar iron abundances are plotted in Fig. 1, based on the data of [10]; low-metallicity ($[\mathrm{Fe/H}] \approx -0.5 - -2.0$) R CrB stars are plotted based on the data of [11]. The overabundance of oxygen in R CrB stars reaches nearly two orders of magnitude, and may be nearly independent of [Fe/H] (Fig. 1). The reason for the overabundance of O and C in R CrB stars is the episodic penetration of the convective envelope of the star on the asymptotic giant branch onto the layer enriched in the products of helium burning [22]. This process enhances the observed abundances of C, O, and N in red supergiants by nearly two orders of magnitude. This oxygen-enrichment mechanism is possible only for red (super)giants with luminosities that are more than two orders of magnitude higher than the solar luminosity. Stars of lower mass may become enriched in carbon or oxygen due to mass exchange between the components of close binaries. This may explain the origin of such oxygen-rich stars as LP 625-44 and CS 29497-030 [14]. Stars with carbon abundances [C/Fe] = 2 and [Fe/H] $= -4$ are known [23].

An increasing number of observations of stars with $[\mathrm{Fe/H}] < -3$ have been reported in recent years. The very low metallicities of these stars reflect the earliest stages of the evolution of the Galaxy [24]. Such stars can be arbitrarily separated into two groups (Fig. 1). The first group contains stars that show a substantial excess of oxygen relative to the model: G 77-61 [15], CS 29498-043 [14], CS 22949-037 [13], CS 22957-027 [25] ($[\mathrm{O/Fe}] \approx 2$, $[\mathrm{Fe/H}] = -3.11$), and CS 31062-012 [25] ($[\mathrm{O/Fe}] \approx 2$, $[\mathrm{Fe/H}] = -2.55$), and R CrB. The second group contains the giant HE 0107-5240 [12]. While the O excesses in stars of the first group can be explained by the penetration of their convective envelopes into the layer enriched in oxygen or by mass exchange between binary components, of the oxygen overabundance in the stars with the lowest metallicities may be primordial, indicating that they formed during the first $\sim 10^7$ yr of the Galaxy's existence. Figure 1 shows that the [O/Fe] ratio in the earliest stages of the Galaxy's evolution is very high, and decreases with age. Since SN Ia have not yet started to enrich the interstellar medium in iron, a natural question arises: What is the reason for this behaviour of [O/Fe]?

The reason for the increase of the [O/Fe] ratio is the increase in the production of oxygen and the decrease in the production of iron with increasing initial masses of SN II precursors. According to the numerical models [26, 27], the amount of oxygen M_O produced by stars with masses of 15–120 $M_\odot$ can be written

$$\frac{M_\mathrm{O}}{M_\odot} = 0.01 \left(\frac{M_\mathrm{i}}{M_\odot}\right)^{1.7},$$

where M_i is the initial mass of the star. The amount of iron produced by 13–25 $M_\odot$ stars can be estimated as [27]

$$\frac{M_\mathrm{Fe}}{M_\odot} = 21 \left(\frac{M_\mathrm{i}}{M_\odot}\right)^{-1.87}.$$

Combining these relations, we obtain

$$\frac{M_\mathrm{O}}{M_\mathrm{Fe}} \approx 5 \times 10^{-4} \left(\frac{M_\mathrm{i}}{M_\odot}\right)^{3.57}. \qquad (1)$$

This expression is valid for $13 < M_\mathrm{i}/M_\odot < 120$, since only stars of these masses were studied in [26, 27]. Of course, when working with (1), we must bear in mind that, while the production of oxygen by massive stars is estimated relatively accurately, the iron yield remains uncertain. It may depend on several parameters that are not accurately known, such as the initial chemical composition of the stars, the rotational velocity of the presupernova core, the magnetic-field strength etc. It is clear from observations that the iron yield may be even smaller than the models [27] predict. For instance, SN 1997D, with a total mass of $\sim 25 M_\odot$, ejected only $2 \times 10^{-3} M_\odot$ of nickel (which produces iron as it decays) [28], much less than the $\sim 0.05 M_\odot$ expected from the models [27]. On the other hand, SN 2002ap, with an initial mass of $\sim 25 M_\odot$, produced $0.07 M_\odot$ of nickel [29], close to the model expectations.

According to (1), obtaining the ratio $[\mathrm{O/Fe}] \approx 2$ observed in the extreme low-metallicity star HE 0107-5240 (Fig. 1) requires a supernova with an initial mass of $\sim 50 M_\odot$ and an age of 3×10^6 yr. Thus, judging from the iron abundance, HE 0107-5240 is among the first stars to be formed in the Galaxy, during the first several million years of its existence. Stars with $[\mathrm{Fe/H}] \lesssim -3$ have masses of the order of a solar mass. This suggests that the initial enrichment of the Galaxy in heavy elements was accomplished by ordinary stars with masses from $\sim 1M_\odot$ to $\sim 100M_\odot$.

The metallicity of the first Galactic stars could grow due to the accretion of interstellar gas. If the radius for capturing interstellar gas by a star is $r = 2GMv^{-2}$, where G is the gravitational constant, M the mass of the star, and v its relative velocity, the star can accrete during the lifetime of the Galaxy a mass

$$\frac{\Delta M}{M_\odot} \approx 10^{-5}\frac{n_{\rm H}}{v_{30}^3}, \qquad (2)$$

where $n_{\rm H}$ is the current number density of the hydrogen in the gaseous phase (in cm^{-3}) and v is the relative velocity (in units of 30 km/s). According to (2), even in stars that are completely devoid of heavy elements, the relative iron abundance could become equal to that observed in HE 0107-5240 (Fig. 1) due to accretion (if there is a negligible role of the stellar wind, low mixing efficiency in the outer layers of the star, etc.). Note that low-metallicity stars could have initially belonged to a former low-mass satellite that merged with the Galaxy in the past. The evolution of the chemical composition of low-mass spheroidal galaxies may end in an early phase, after loss of the gaseous component. Naturally, stars in such a galaxy could retain their high [O/Fe] values.

For completeness, we note an additional possible means of enrichment of population-III low-mass stars (which are initially devoid of heavy elements) in metals. Most stars are formed in stellar clusters, which, as a rule, are disrupted almost immediately after their formation because of the loss of the gaseous component due to the formation of HII regions and supernova explosions [31]. The first stars may also have formed in clusters. Then, some fraction of the lost gas, along with the products of the first, most massive, supernovae, would be captured by low-mass stars with the initial low-metal chemical composition. The capture radius is $r \approx 2GM_*v_{\rm ex}^{-2}$, where $M_* \approx M_\odot$ is the mass of the cluster star and $v_{\rm ex}$ the velocity of the expanding gaseous envelope of the cluster. The fraction of the captured matter will then be

$$\alpha = \frac{G^2M_*^2}{v_{\rm ex}^4R^2} = \left(\frac{v_{\rm ff}}{v_{\rm ex}}\right)^4 N^{-2}, \qquad (3)$$

where R is the cluster radius, $v_{\rm ff}$ the free-fall velocity at the edge of the cluster, and N the number of stars in the cluster (assuming that all have the solar mass). If we assume that $v_{\rm ff} = v_{\rm ex}$, $N = 10^3$ and $M_{\rm Fe} \approx 0.01\ M_\odot$ ($M_{\rm O} \approx 50\ M_\odot$ [27])), then a solar-mass star can capture $\sim 10^{-8}M_\odot$ of iron. This produces a star with an iron abundance of [Fe/H] ≈ -5, similar to that observed in HE 0107-5240 (Fig. 1). It is obvious that a high oxygen abundance will be observed, since stars with masses exceeding $\sim 50M_\odot$ have [O/Fe] ≈ 2, as was shown above. Note that not all the parameters in (3) are well enough known to enable confident conclusions about the role of this mechanism in the enrichment of population-III stars in heavy elements. The accretion of interstellar gas enriched in heavy elements produced by the first stars may substantially complicate, or even make impossible, the identification of low-mass population-III stars.

Note that the [O/Fe]–[Fe/H] evolutionary curve obtained for the closed model shown in Fig. 1 represents an upper bound for the oxygen abundance. In low-mass disk galaxies, the products of SN II explosions can efficiently leave the parent galaxies via the formation of supershells [32], thereby reducing the growth rate of the oxygen abundance in these galaxies. Since type Ia supernovae do not produce supershells, the iron abundance in low-mass disk galaxies increases at the usual pace. The example provided by the galaxy IZw 18 [33], which has active star formation with [Fe/H] $= -1.76 \pm 0.12$ and [O/Fe] $= -0.3 \pm 0.3$, shows that the loss of the products of type II supernovae may,

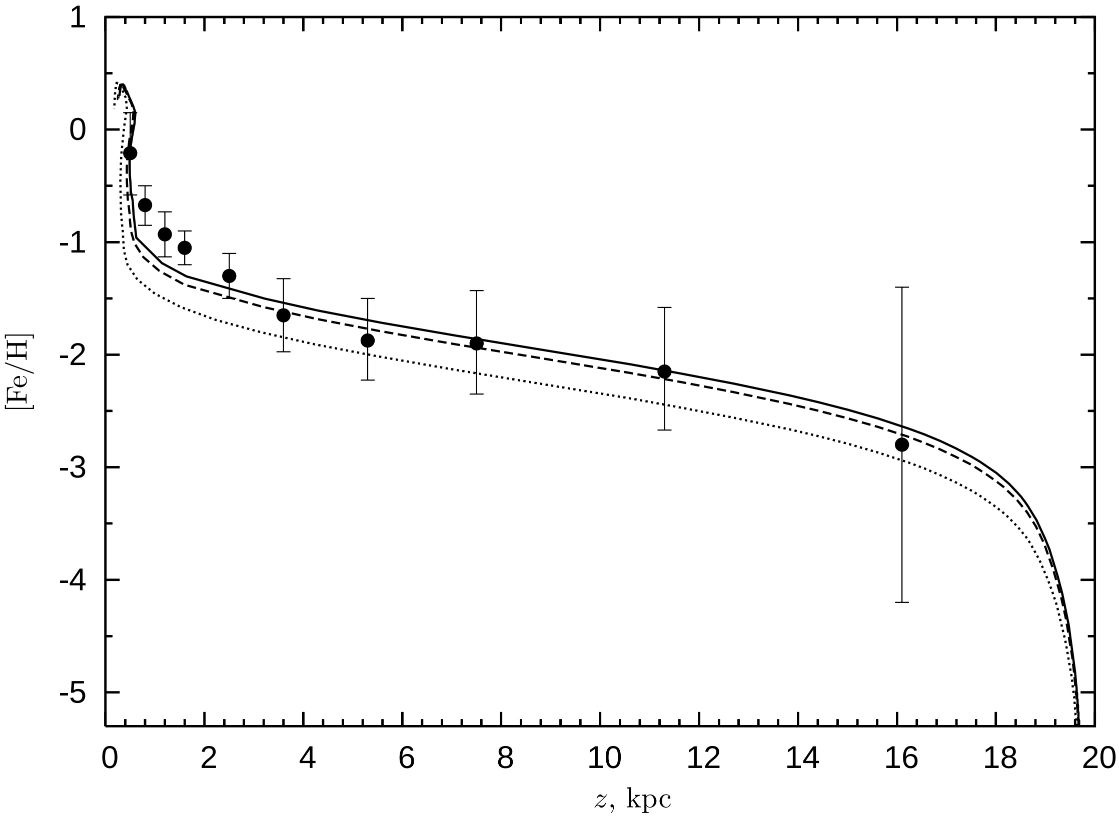

FIG. 2: Distribution of iron abundance with height above the Galactic plane in the standard model (solid curve) and in a model taking into account the loss of heavy elements due to SN II explosions, for fractional masses of heavy elements lost equal to 0.16 (dashed curve) and 0.5 (dotted curve). The solid circles show the data from [30].

indeed, be very important for dwarf galaxies. As our model computations show, allowing for the loss of type I supernova products in massive galaxies does not lead to any substantial differences in the [O/Fe]–[Fe/H] distribution. Moreover, special runs of the model taking into account the finite time for the accumulation of the Galactic matter show that increasing the Galaxy's formation time substantially reduces the [O/Fe] ratio at low [Fe/H] (Fig. 1). Increasing the amount of data on low-metallicity stars in the future may enable estimation of the time for the accumulation of the Galaxy's mass.

III. DISTRIBUTION OF HEAVY ELEMENTS ABOVE THE GALACTIC DISK

Let us now consider the distribution of heavy elements with height z above the Galactic disk. Various observations show that the metallicity gradient with z measured using field stars may reach -0.65/kpc (according to data for the thin disk [34])), while the lowest value obtained from observations of open clusters is -0.34/kpc [35]. At the same time, some observations of field and open-cluster stars show no evidence for a metallicity gradient [36, 37]. To summarize, at $z < 4$ kpc, the gradient is in the range $(-0.55\ldots-0.33)$/kpc, while it is in the range $(-0.18\ldots0)$/kpc at larger z [30].

In the standard model, we adopted the

TABLE I: Evolution of the main parameters of the standard Galaxy model with age (SFR is the star formation rate in $M_\odot$/yr, H_g the semi-thickness of the gaseous disk, M_g the mass of the gas, Z the fractional mass of heavy elements, τ_dust the optical depth of the dust, $L_\mathrm{opt} = L_\mathrm{bol}/\tau_\mathrm{dust}(1 - e^{-\tau_\mathrm{dust}})$ the optical luminosity with allowance for absorption by dust)

t, yr	SFR	H_g, pc	$M_\mathrm{g}/M_\odot$	Z	[O/H]	[Fe/H]	τ_dust	$L_\mathrm{opt}/L_\odot$	$L_\mathrm{bol}/L_\odot$
$3.6 \cdot 10^6$	34.3	$2.0 \cdot 10^4$	$2.0 \cdot 10^{11}$	$7.0 \cdot 10^{-7}$	−4.4	−6.9	0.0012	$1.1 \cdot 10^{10}$	$1.1 \cdot 10^{10}$
$4.8 \cdot 10^6$	34.4	$2.0 \cdot 10^4$	$2.0 \cdot 10^{11}$	$2.0 \cdot 10^{-6}$	−3.9	−5.8	0.0034	$1.2 \cdot 10^{10}$	$1.2 \cdot 10^{10}$
$6.3 \cdot 10^6$	34.5	$2.0 \cdot 10^4$	$2.0 \cdot 10^{11}$	$4.3 \cdot 10^{-6}$	−3.6	−5.1	0.0072	$1.3 \cdot 10^{10}$	$1.3 \cdot 10^{10}$
$8.2 \cdot 10^6$	34.7	$2.0 \cdot 10^4$	$2.0 \cdot 10^{11}$	$7.5 \cdot 10^{-6}$	−3.4	−4.7	0.0012	$1.3 \cdot 10^{10}$	$1.4 \cdot 10^{10}$
$1.0 \cdot 10^7$	34.9	$1.9 \cdot 10^4$	$2.0 \cdot 10^{11}$	$1.2 \cdot 10^{-5}$	−3.2	−4.3	0.020	$1.4 \cdot 10^{10}$	$1.4 \cdot 10^{10}$
$1.5 \cdot 10^7$	35.3	$1.9 \cdot 10^4$	$2.0 \cdot 10^{11}$	$2.2 \cdot 10^{-5}$	−3.0	−3.8	0.036	$1.5 \cdot 10^{10}$	$1.6 \cdot 10^{10}$
$2.5 \cdot 10^7$	36.2	$1.9 \cdot 10^4$	$2.0 \cdot 10^{11}$	$4.3 \cdot 10^{-5}$	−2.7	−3.3	0.071	$1.7 \cdot 10^{10}$	$1.7 \cdot 10^{10}$
$3.4 \cdot 10^7$	37.0	$1.8 \cdot 10^4$	$2.0 \cdot 10^{11}$	$6.3 \cdot 10^{-5}$	−2.5	−3.1	0.10	$1.8 \cdot 10^{10}$	$1.9 \cdot 10^{10}$
$4.4 \cdot 10^7$	37.9	$1.8 \cdot 10^4$	$2.0 \cdot 10^{11}$	$8.4 \cdot 10^{-5}$	−2.4	−3.0	0.14	$1.9 \cdot 10^{10}$	$2.0 \cdot 10^{10}$
$6.0 \cdot 10^7$	39.5	$1.7 \cdot 10^4$	$2.0 \cdot 10^{11}$	$1.2 \cdot 10^{-4}$	−2.3	−2.8	0.20	$2.0 \cdot 10^{10}$	$2.2 \cdot 10^{10}$
$7.3 \cdot 10^7$	40.9	$1.6 \cdot 10^4$	$2.0 \cdot 10^{11}$	$1.5 \cdot 10^{-4}$	−2.2	−2.7	0.25	$2.0 \cdot 10^{10}$	$2.3 \cdot 10^{10}$
$9.8 \cdot 10^7$	43.8	$1.5 \cdot 10^4$	$2.0 \cdot 10^{11}$	$2.2 \cdot 10^{-4}$	−2.0	−2.5	0.36	$2.2 \cdot 10^{10}$	$2.6 \cdot 10^{10}$
$1.2 \cdot 10^8$	47.0	$1.4 \cdot 10^4$	$2.0 \cdot 10^{11}$	$3.0 \cdot 10^{-4}$	−1.9	−2.4	0.47	$2.3 \cdot 10^{10}$	$2.9 \cdot 10^{10}$
$1.7 \cdot 10^8$	54.6	$1.2 \cdot 10^4$	$1.9 \cdot 10^{11}$	$4.4 \cdot 10^{-4}$	−1.7	−2.2	0.72	$2.5 \cdot 10^{10}$	$3.5 \cdot 10^{10}$
$2.5 \cdot 10^8$	69.7	$8.7 \cdot 10^3$	$1.9 \cdot 10^{11}$	$7.2 \cdot 10^{-4}$	−1.5	−2.0	1.1	$2.7 \cdot 10^{10}$	$4.5 \cdot 10^{10}$
$3.0 \cdot 10^8$	83.3	$7.0 \cdot 10^3$	$1.9 \cdot 10^{11}$	$9.5 \cdot 10^{-4}$	−1.4	−1.8	1.5	$2.9 \cdot 10^{10}$	$5.5 \cdot 10^{10}$
$4.0 \cdot 10^8$	123.7	$4.3 \cdot 10^3$	$1.8 \cdot 10^{11}$	$1.6 \cdot 10^{-3}$	−1.2	−1.6	2.3	$3.2 \cdot 10^{10}$	$8.1 \cdot 10^{10}$
$5.6 \cdot 10^8$	243.5	$1.6 \cdot 10^3$	$1.5 \cdot 10^{11}$	$3.1 \cdot 10^{-3}$	−0.9	−1.3	4.0	$3.6 \cdot 10^{10}$	$1.5 \cdot 10^{11}$
$7.1 \cdot 10^8$	342.7	$6.2 \cdot 10^2$	$1.1 \cdot 10^{11}$	$6.9 \cdot 10^{-3}$	−0.5	−1.0	6.5	$3.8 \cdot 10^{10}$	$2.5 \cdot 10^{11}$
$9.2 \cdot 10^8$	161.7	$5.5 \cdot 10^2$	$7.2 \cdot 10^{10}$	$1.4 \cdot 10^{-2}$	−0.2	−0.6	8.6	$2.4 \cdot 10^{10}$	$2.0 \cdot 10^{11}$
$1.2 \cdot 10^9$	76.1	$4.9 \cdot 10^2$	$4.7 \cdot 10^{10}$	$2.1 \cdot 10^{-2}$	0.0	−0.4	8.2	$1.6 \cdot 10^{10}$	$1.3 \cdot 10^{11}$
$1.6 \cdot 10^9$	33.7	$5.4 \cdot 10^2$	$3.3 \cdot 10^{10}$	$2.7 \cdot 10^{-2}$	0.0	0.0	7.4	$1.2 \cdot 10^{10}$	$8.9 \cdot 10^{10}$
$2.1 \cdot 10^9$	21.1	$5.0 \cdot 10^2$	$2.5 \cdot 10^{10}$	$3.3 \cdot 10^{-2}$	0.1	0.3	6.8	$9.8 \cdot 10^9$	$6.7 \cdot 10^{10}$
$2.9 \cdot 10^9$	12.8	$4.1 \cdot 10^2$	$1.8 \cdot 10^{10}$	$3.8 \cdot 10^{-2}$	0.1	0.4	5.6	$9.5 \cdot 10^9$	$5.3 \cdot 10^{10}$
$3.8 \cdot 10^9$	7.2	$3.8 \cdot 10^2$	$1.3 \cdot 10^{10}$	$4.2 \cdot 10^{-2}$	0.2	0.4	4.4	$9.4 \cdot 10^9$	$4.2 \cdot 10^{10}$

value of [Fe/H] as a function of the disk semi-thickness for the dependence of the iron abundance on the height above the Galactic plane. This dependence is shown in Fig. 2, along with data from [30]. We can distinguish three regions with different metallicity gradients: d[Fe/H]$/dz = -3$/kpc for $z < 0.7$ kpc, d[Fe/H]$/dz = -0.2$/kpc for $0.7 < z < 5$ kpc, and d[Fe/H]$/dz = -0.1$/kpc for $5 < z < 16$ kpc. This corresponds to different iron abundances in stars of the thin disk, thick disk, and halo, and also to different spatial scales within these components.

Computations of galactic evolution allowing for the loss of heavy elements (Fig. 2) and accretion have shown that the “openness” of the galaxy weakly influences the model dependence of [Fe/H] on z. Thus, our one-zone model can explain well the variations of the distribution of heavy elements with z.

IV. EVOLUTION OF A DISK GALAXY: THE INFLUENCE OF DARK MATTER

The main results obtained for the standard model are listed in the table. Comparison with observations indicates that this model provides an adequate description of the chemical and dynamical evolution of the Galaxy, as well as of its star-formation history. For example, the data of [38] provide evidence that young galaxies with $\dot{M}_* \approx$ 10–100$M_\odot$/yr have optical depths of $\sim$ 5–10 in the direction perpendicular to the plane of the disk, as is confirmed by our model. The large optical depths of distant, and thus young, galaxies could influence the extragalactic distance scale (which is based on the assumption that SN Ia are standard candles), and therefore conclusions concerning the regime of the cosmological expansion. We should also bear this in mind in connection with analyses of the brightness of supernovae at $z = 2$–5. Variation of the time to accumulate the mass of the Galaxy in the initial stage of its formation did not influence substantially the Galaxy's parameters after the Hubble time (Fig. 1).

Our model has another important parameter — the mass of dark matter, i.e., of matter (baryonic or otherwise) that cannot be directly observed, but provides a (sometimes dominant) contribution to the gravitational field. The fractional mass of dark matter is small on small scales. For instance, estimates of the fractional mass of dark matter in the Sun yield less than 2–5% [39], and this is probably true for other stars as well. On scales of 100 kpc or more, the fractional mass of dark matter may be much larger [16].

We studied the role of dark matter in the evolution of the Galaxy by changing the expression for the gravitational potential in the standard model to

$$E = \frac{GM_\mathrm{g}H_\mathrm{g}^2}{R^2}\left(\frac{M_\mathrm{G}}{H_*} + \frac{M_\mathrm{dm}}{R}\right),$$

where G is the gravitational constant, M_g the mass of gas, H_g the semi-thickness of the gaseous disk, M_G the mass of visible matter, H_* the semi-thickness of the stellar disk, M_dm the mass of dark matter, and R the radius of the disk. Figure 3 shows the evolution of the main parameters of the Galaxy as functions of the ratio of the masses of dark and visible matter, which was varied from zero (corresponding to the standard model) to two. Reduction of the mass of matter involved in star formation results in a delay of the star-formation burst, and so reduces the thickness of the gaseous disk. This is in qualitative agreement with estimates following from the observational relation between the relative thickness of the disk and the mass–luminosity relation for galaxies [40]. Increasing the mass-to-luminosity ratio in the model decreases the galaxy's relative thickness. The observed optical luminosity of the Galaxy places constraints on the fractional mass of dark matter, $< 50\%$. Note that our initial mass function, $dN \propto M^{-2.35}dM$ for $M > 0.1\ M_\odot$, overestimates the number of low-mass stars compared to the observed value. According to [41], the observed mass function changes slope at $M \approx 1M_\odot$ ($dN \propto M^{-1.5}dM$ for $M < 1M_\odot$), which makes the fraction of stars with $< 1M_\odot$ less pronounced. Thus, an excess of matter appears in our model compared to the observations. A simple analytical estimate of its fractional mass is $\sim 37\%$.

V. TULLY–FISHER RELATION

About a quarter of a century ago, Tully and Fisher [17] discovered a dependence between the luminosity of a disk galaxy and its rotational velocity. In modern form, this relation can be written

$$\Delta M_\mathrm{B} = (8 \pm 1)\Delta \log v_\mathrm{rot}, \qquad (4)$$

where M_B is the absolute B magnitude of the galaxy and v_rot is the rotational velocity of the galactic disk, estimated from the flat

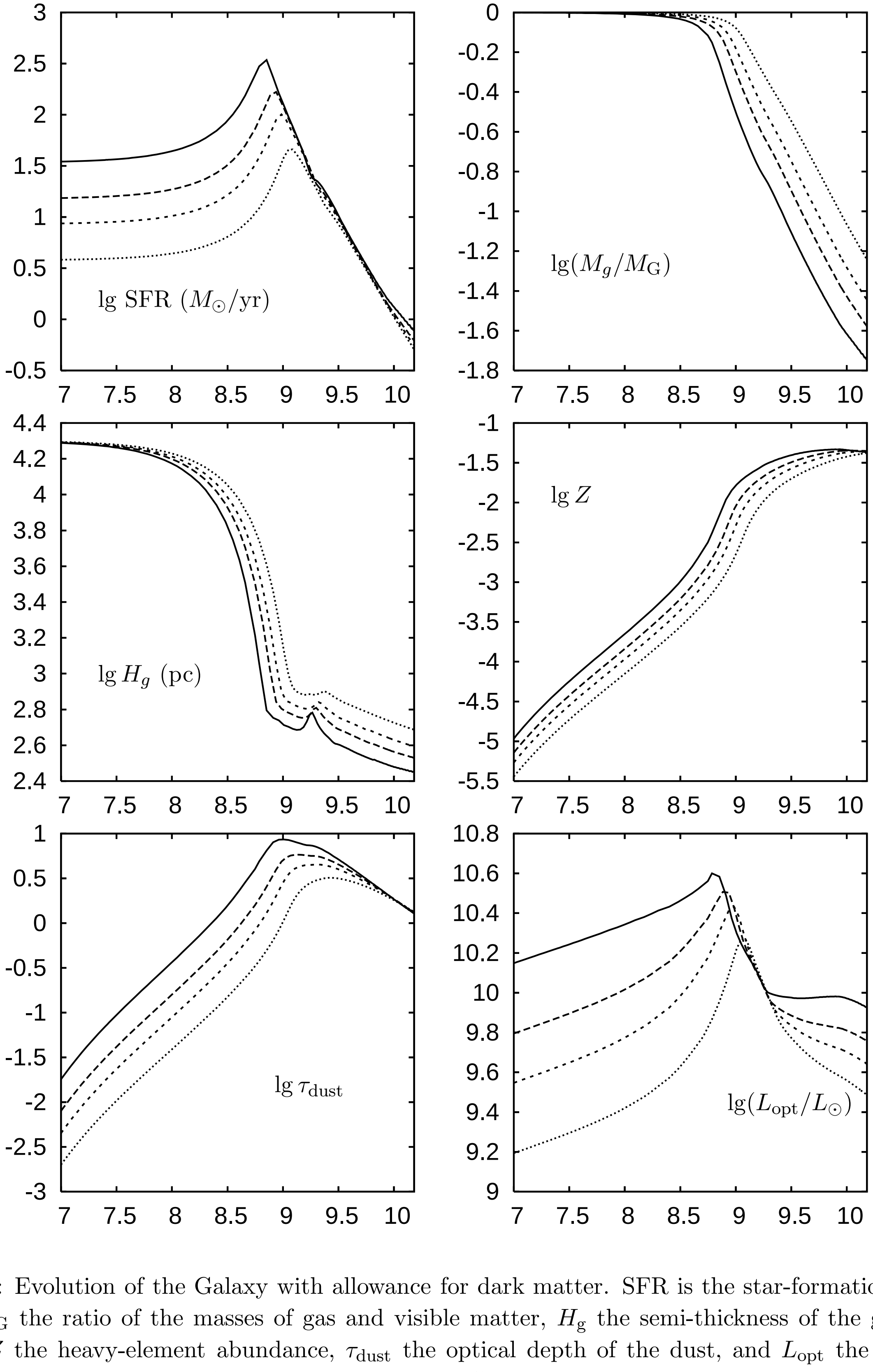

FIG. 3: Evolution of the Galaxy with allowance for dark matter. SFR is the star-formation rate, M_g/M_G the ratio of the masses of gas and visible matter, H_g the semi-thickness of the gaseous disk, Z the heavy-element abundance, τ_{dust} the optical depth of the dust, and L_{opt} the optical luminosity with allowance for absorption by dust. Computational results are shown for ratios of the masses of dark and visible matter M_{dm}/M_G equal to 0 (solid curve), 0.5 (long dashed curve), 1.0 (short-dashed curve), and 2.0 (dotted curve).

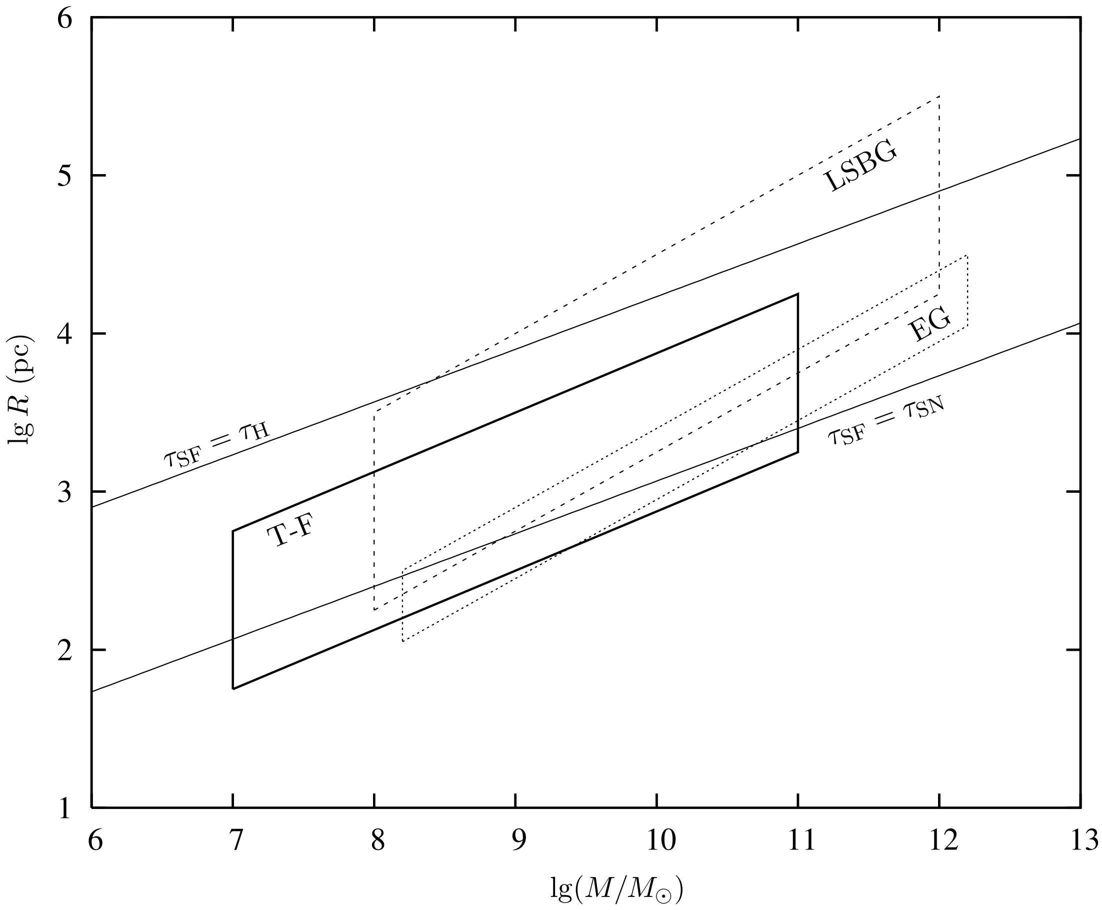

FIG. 4: Mass–radius diagram for various galaxies; galaxies obey the Tully–Fisher relation in the region T–F. The lines $\tau_{\rm SF} = \tau_{\rm SN}$ and $\tau_{\rm SF} = \tau_{\rm Hubble}$ define the positions of galaxies with star-formation timescales $\tau_{\rm SF}$ and $\tau_{\rm H}$, respectively. The region LSBG is occupied by low-surface-brightness galaxies [42, 43]. Early-type galaxies are located in the region EG [44, 45] (see Sect. 5).

part of the rotation curve. We can use the mass–luminosity relation for disk galaxies, $M/M_\odot \sim 10L/L_\odot$ [46], to estimate the relation between the mass of a disk galaxy M and its radius R. Assuming $v_{\rm rot} \propto M^{1/2}R^{-1/2}$, we obtain

$$R \propto M^{0.5\pm0.07} \,. \tag{5}$$

Relations similar to (4) for varioius groups of disk galaxies have been studied by numerous authors (see, e. g., [47, 48, 49]). If selection effects are not considered, it appears that the locations and slopes of the $\log R$–$logM$ relation derived from (4) are fairly uncertain (they vary by about a factor of three for galaxies with masses from 10^7 to $10^{11} M_\odot$). The Tully–Fisher relation can be written $M = \pi\Sigma R^2$, where Σ is the surface density of gravitating matter. The observed range of Σ is rather wide. According to [42], disk galaxies display values $\Sigma \approx 10$–$600\ M_\odot/{\rm pc}^2$; another estimate yields $\Sigma = 20$–$1500 M_\odot/{\rm pc}^2$ [50]. Figure 4 plots a mass–radius diagram for galaxies of various types that obey the Tully–Fisher relation (located inside the “T–F” region in this figure), elliptical and early-type galaxies (EG; [44, 45]), and low-surface-density galaxies (LSBG; [42, 43]).

We used (5) to compute a series of models with masses of $10^6 - 4.5 \times 10^{11} M_\odot$. The results show that, in this range, the mass of a galaxy exerts almost no influence on the star-formation history or the evolution of the chemical composition. In particular, the final heavy-element abundance does not depend on the mass, in contradiction with the observed increase of the heavy-element abundance with increasing galactic mass and luminosity [51]. This may be explained by the loss of heavy elements by low-mass galaxies.

Our formalism [2, 3] enables us to derive a simple relation defining the time scale for star formation in a spherical galaxy [52]:

$$\tau_{\mathrm{SF}} = 3 \times 10^8 \frac{R_4^3}{M_{11}},$$

where R_4 is the galactic radius in units of 10^4 pc and M_{11} the mass of its gaseous component in units of $10^{11} M_\odot$. The observed masses and radii of young galaxies are consistent with $\tau_{\mathrm{SF}} = 10^7$–$10^9$ yr [53]. The spherical model describes the early stages of the evolution of disk galaxies. We can place limits on the time for the existence of star-forming galaxies. An upper bound for the region they can occupy in Fig. 4 is given by the Hubble time: $\tau_{\mathrm{SF}} = \tau_{\mathrm{H}} = 1.4 \times 10^{10}$ yr, as is shown in Fig. 4. In galaxies located above this line, the SFR is so low that only a small fraction of the gas has been turned into stars over the Hubble time. Note that the position of this bound virtually coincides with the position occupied by low-surface-brightness galaxies [42, 43]. Nearby galaxies with masses of 10^6–$10^{12} M_\odot$ from the catalog [54] abut on the upper boundary of the region of star-forming galaxies (they are not shown in Fig. 4); the star-formation time scale in such galaxies is $\tau_{\mathrm{SF}} \approx 80^9$–$10^{10}$ yr.

On the other hand, the SFR in high-density galaxies is so high that almost all the gas has been transformed into stars even before the first explosions of SN II, whose precursors have lifetimes $\tau_{\mathrm{SN}} \approx 5 \times 10^6$ yr. This corresponds to the relation $\tau_{\mathrm{SN}} < \tau_{\mathrm{SF}}$, or $M_{11} > 60 R_4^3$ (the line $\tau_{\mathrm{SN}} = \tau_{\mathrm{SF}}$ is also plotted in Fig. 4). As soon as the SN II begin to explode in these galaxies, they clean out any remaining gas. This is the scenario for the evolution for elliptical galaxies. The mass lost by old stars in these galaxies is unable to revive star formation, since SN Ia explosions drive the galactic wind, hindering star formation throughout the galaxy, with the possible exception of a circumnuclear region with a high gas density (see, for example, [55]). In fact, only a few percent of S0 and E galaxies show signs of star formation in their nuclei [56]. Some S0 and E galaxies may form via collisions of disk galaxies [57, 58]. However, the number of such galaxies is not large, since observations [59] show only a small increase in the fraction of E galaxies with the age of Universe; hence, most formed at large redshifts. Albeit with a fairly large scatter, the positions of early-type galaxies in Fig. 4 are close to the boundary defined by the relation $\tau_{\mathrm{SF}} = \tau_{\mathrm{SN}}$. However, elliptical galaxies formed in collisions of disk galaxies may also have larger sizes.

Figure 4 shows that the galaxies with active continuing star formation are located in a strip defined by the conditions $\tau_{\mathrm{SN}} = \tau_{\mathrm{SF}}$ and $\tau_{\mathrm{SN}} = \tau_{\mathrm{H}}$; the slope of this strip is close to the slope of the Tully–Fisher relation. This suggests that the power of the $R \propto M^\alpha$ law is determined by the similarity of the slopes of the boundaries of the region occupied by disk galaxies in the mass–radius diagram. At the lower boundary of this zone, galaxies that are initially elliptical are formed, while the upper boundary is apparently defined by two circumstances. The first is the condition that there be a sufficient SFR on a time scale that is shorter than the Hubble time. The second is the near coincidence of the upper boundary with the position of galaxies that have surface brightnesses at the detection limit. Galaxies with lower surface densities, $\Sigma < 10 M_\odot/\mathrm{pc}^2$, are probably not detectable.

VI. CONCLUSION

Our study of the evolution of a disk galaxy with star formation governed by ionization has enabled us to apply this model to several new fields. In particular, we have shown that high oxygen-to-iron abundance ratios are characteristic of the very first stars formed: [O/Fe] ≈ 2 when [Fe/H] $\lesssim -5$. This is a result of the reduction in the iron production and increase in the oxygen production with increasing initial mass of type II supernovae. This suggests that some stars with low iron abundances and relatively high oxygen abundances (G 77-61, HE 0107-5240, Fig. 1) may be either the earliest second-generation stars or first-generation stars that are "contaminated" by products of the first supernovae. Our model distribution of metals with height z above the Galactic disk agrees with the observed distribution to $z \sim 16$ kpc. In our model, the well-known Tully–Fisher relation may stem from a combination of observational selection effects and conditions that are necessary for the formation of disk galaxies.

VII. ACKNOWLEDGMENTS

This study was supported by the Presidential Program "Leading Scientific Schools of Russia" (NSh-162.2003.2), the Russian Foundation for Basic Research (project codes 02-02-17524, 03-02-162254), and the Program of the Physical Sciences Branch of the Russian Academy of Sciences "Extended Objects in the Universe."

[1] D. Z. Wiebe, A. V. Tutukov, and B. M. Shustov, Astron. Rep. **42**, 1 (1998).

[2] C. Firmani and A. Tutukov, Astron. and Astrophys. **264**, 37 (1992).

[3] C. Firmani and A. Tutukov, Astron. and Astrophys. **288**, 713 (1994).

[4] D. Wiebe, B. Shustov, and A. Tutukov, Astron. and Astrophys. **345**, 93 (1999).

[5] D. Wiebe, A. Moiseev, and A. Tutukov, Astron. Rep.(in press) **2005** (2005).

[6] P. Thorén, B. Edvardsson, and B. Gustafsson, Astron. and Astrophys. **425**, 187 (2004).

[7] P. E. Nissen, F. Primas, M. Asplund, and D. L. Lambert, Astron. and Astrophys. **390**, 235 (2002).

[8] G. Israelian, R. Rebolo, R. J. García López, P. Bonifacio, P. Molaro, G. Basri, and N. Shchukina, Astrophys. J. **551**, 833 (2001).

[9] B. Barbuy, Astron. and Astrophys. **191**, 121 (1988).

[10] G. Pandey, N. Kameswara Rao, D. L. Lambert, C. S. Jeffery, and M. Asplund, Monthly Not. Roy. Astron. Soc. **324**, 937 (2001).

[11] N. K. Rao (2004), astro-ph/0410648.

[12] M. S. Bessell, N. Christlieb, and B. Gustafsson, Astrophys. J. (Letters) **612**, L61 (2004).

[13] R. Cayrel, E. Depagne, M. Spite, V. Hill, F. Spite, P. François, B. Plez, T. Beers, F. Primas, J. Andersen, et al., Astron. and Astrophys. **416**, 1117 (2004).

[14] G. Israelian, N. Shchukina, R. Rebolo, G. Basri, J. I. González Hernández, and T. Kajino, Astron. and Astrophys. **419**, 1095 (2004).

[15] B. Plez and J. G. Cohen (2005), astro-ph/0501535.

[16] B. M. Shustov, in *Proc. 34th International Student Science Conference on Physics of the Cosmos* (Ural'skii Univ., Ekaterinburg, 2005), p. 207.

[17] R. B. Tully and J. R. Fisher, Astron. and Astrophys. **54**, 661 (1977).

[18] I. J. Iben and A. Tutukov, Astrophys. J. Suppl. Ser. **54**, 335 (1984).

[19] A. V. Tutukov and L. R. Yungel'son, Astron. Rep. **46**, 1 (2002).

[20] A. J. Barth, P. Martini, C. H. Nelson, and L. C. Ho, Astrophys. J. (Letters) **594**, L95 (2003).

[21] T. Bensby, S. Feltzing, and I. Lundström,

Astron. and Astrophys. **415**, 155 (2004).

[22] I. J. Iben and A. Renzini, Ann. Rev. Astron. and Astrophys. **54**, 271 (1983).

[23] S. G. Ryan (2002), astro-ph/0211608.

[24] T. Suda, M. Aikawa, and M. Machida, Astrophys. J. **611**, 476 (2004).

[25] H. Umeda and K. Nomoto, Astrophys. J. **619**, 445 (2005).

[26] A. Maeder, Astron. and Astrophys. **264**, 105 (1992).

[27] F. Tielemann, K. Nomoto, and M. Hashimoto, Astrophys. J. **460**, 408 (1996).

[28] H. Umeda and K. Nomoto, Nature **422**, 871 (2003).

[29] P. A. Mazzali, J. Deng, K. Maeda, K. Nomoto, H. Umeda, K. Hatano, K. Iwamoto, Y. Yoshii, Y. Kobayashi, T. Minezaki, et al., Astrophys. J. (Letters) **572**, L61 (2002).

[30] C. Du, X. Zhou, J. Ma, J. Shi, A. B. Chen, Z. Jiang, and J. Chen, Astron. J. **128**, 2265 (2004).

[31] A. V. Tutukov, Astron. and Astrophys. **70**, 57 (1978).

[32] I. V. Igumenshchev, B. M. Shustov, and A. V. Tutukov, Astron. and Astrophys. **30**, 524 (1990).

[33] A. Aloisi, S. Savaglio, T. M. Heckman, C. G. Hoopes, C. Leitherer, and K. R. Sembach, Astrophys. J. **595**, 760 (2003).

[34] T. Yamagata and Y. Yoshii, in *IAU Symp. 161: Astronomy from Wide-Field Imaging* (1994), pp. 420–+.

[35] G. Carraro, Y. K. Ng, and L. Portinari, Monthly Not. Roy. Astron. Soc. **296**, 1045 (1998).

[36] G. Gilmore and R. F. G. Wyse, Astron. J. **90**, 2015 (1985).

[37] E. D. Friel, Ann. Rev. Astron. and Astrophys. **33**, 381 (1995).

[38] Y. C. Liang, F. Hammer, H. Flores, D. Elbaz, D. Marcillac, and C. J. Cesarsky, Astron. and Astrophys. **423**, 867 (2004).

[39] N. Kardashov, A. Tutukov, and A. Fedorova, Astron. Rep. **49** (2005).

[40] A. V. Zasov, D. V. Bizyaev, D. I. Makarov, and N. V. Tyurina, Astronomy Letters **28**, 527 (2002).

[41] P. Kroupa and C. M. Boily, Monthly Not. Roy. Astron. Soc. **336**, 1188 (2002).

[42] A. Y. Kniazev, E. K. Grebel, S. A. Pustilnik, A. G. Pramskij, T. F. Kniazeva, F. Prada, and D. Harbeck, Astron. J. **127**, 704 (2004).

[43] K. Okoshi and M. Nagashima (2004), astro-ph/0412561.

[44] S. De Rijcke, D. Michielsen, H. Dejonghe, W. W. Zeilinger, and G. K. T. Hau (2004), astro-ph/0412553.

[45] C. J. Walcher, R. P. van der Marel, D. McLaughlin, H.-W. Rix, T. Boeker, N. Haering, L. C. Ho, M. Sarzi, and J. C. Shields (2004), astro-ph/0409216.

[46] I. D. Karachentsev and A. M. Kut'kin (2004), astro-ph/0412369.

[47] S. J. Kannappan and E. J. Barton, Astron. J. **127**, 2694 (2004).

[48] L. S. Pilyugin, J. M. Vílchez, and T. Contini, Astron. and Astrophys. **425**, 849 (2004).

[49] D. R. Andersen and M. A. Bershady, Astrophys. J. (Letters) **599**, L79 (2003).

[50] D. Pfenniger and Y. Revaz, in *The Dusty and Molecular Universe: A Prelude to Herschel and ALMA, meeting held in Paris, France, October 27-29, 2004, Eds.: A. Wilson. To be published in ESA Conference Series., p.63* (2004), pp. 63–+.

[51] J. J. Salzer et al. (2005), astro-ph/0502202.

[52] A. V. Tutukov, in *Revista Mexicana de Astronomia y Astrofisica Conference Series* (2003), pp. 60–65.

[53] C. Papovich, M. Dickinson, M. Giavalisco, C. J. Conselice, and H. C. Ferguson (2005), astro-ph/0501088.

[54] I. D. Karachentsev, V. E. Karachentseva, W. K. Huchtmeier, and D. I. Makarov, Astron. J. **127**, 2031 (2004).

[55] I. Chilingarian, P. Prugniel, O. Silchenko, and V. Afanasiev (2004), astro-ph/0412293.

[56] M. Fukugita, O. Nakamura, and E. Turner,

Astrophys. J. (Letters) **601**, L127 (2004).

[57] W. Keel and K. Borne, Astron. J. **126**, 1257 (2003).

[58] C. Nipoti, M. Stiavelli, L. Ciotti, T. Treu, and P. Rosati (2003), astro-ph/0311424.

[59] J. A. L. Aguerri and I. Trujillo, Monthly Not. Roy. Astron. Soc. **333**, 633 (2002).